Oscillation and instability of neck propagation in poly(ethylene terephthalate) films

Akihiko Toda
Department of Physics, Faculty of Science, Kyoto University, Kyoto 606, Japan
(Received 4 August 1992; revised 4 October 1992)

The stability of neck propagation and its oscillatory mode have been studied for the cold drawing of poly(ethylene terephthalate) films. On the basis of Barenblatt's model considering a temperature rise at the neck, the stability has been analysed for neck propagation at constant speed and at constant load. It is shown that the stability is directly connected to the sign of the slope of the stress–drawing rate plot; unstable neck propagation should be in the region of negative slope. It is argued that the unstable mode changes to an oscillatory neck propagation for drawing at constant speed, while the mode in drawing at constant load is transformed to the other stable region. Experimental study has confirmed the unstable drawing at constant load and the transition of neck propagation rate. Oscillatory neck propagation has also been examined by a numerical calculation of non-linear differential equations based on Barenblatt's model. The limits of Barenblatt's model are also discussed.

(Keywords: necking; neck propagation; poly(ethylene terephthalate); self-excited oscillation)

INTRODUCTION

Plastic deformation of polymers by cold drawing begins with the formation of a neck and usually proceeds by propagation of the neck. The necking of poly(ethylene terephthalate) (PET) films shows oscillatory propagation; the stress oscillates and the appearance of the sample changes periodically during drawing at constant speed[1] (*Figure 1*). During the oscillation, the following occurs repeatedly[1]: elastic deformation with almost zero velocity of neck propagation and then quick propagation of the neck with elastic shrinkage of the sample. Hence, it is clear that the elastic deformation of the sample is coupled with a certain mechanism of neck propagation, and causes a periodic change in the rate of neck propagation and in the required stress under the constraint of constant drawing speed.

Two different models for the mechanism of oscillatory neck propagation have been proposed to date.

1. Considering a temperature rise caused by the work done at the neck, Barenblatt proposed a mathematical model for the non-isothermal process regarded as a dynamic system in a phase space of stress, drawing velocity and temperature at the neck[2]. The model suggests that the oscillation is due to the instability of a stationary solution changing to a limit cycle; namely, the process is explained as self-excited oscillation.
2. Under the condition of constant load drawing, the same material shows two jumps in the drawing rate at certain critical stresses[3,4] (*Figure 2a*). On the basis of this finding, it has been argued that the oscillation is caused by a cycle comprising two different regions of rates and jumps (*Figure 2a*) and hence the upper and lower critical stresses determine the magnitude of stress oscillation[4]. In this model, the effect of temperature rise at the neck has not been introduced.

The second model cannot explain the following facts. First, under the condition of drawing at constant speed, a region with negative slope exists in the plot of stress (σ) *versus* drawing speed (V)[1], as indicated by region 'b' in *Figure 2b*. The neck propagation in this region remains stable at first but starts oscillating as the extension proceeds (*Figure 1*). The model cannot explain the existence of the stable neck propagation in the early stage. Second, it is also well known that the magnitude of oscillation changes with the speed of drawing[3]: the faster the rate, the smaller the magnitude is (*Figure 2b*). Hence, the magnitude is not directly related to the critical stresses observed under the condition of constant load. Third, it has also been reported that the oscillation and the region

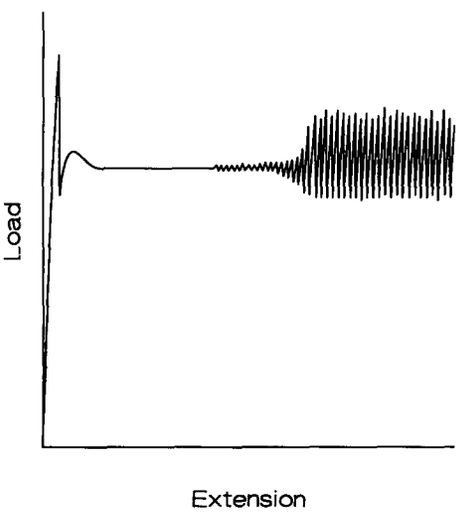

Figure 1 Typical load–extension curve for oscillatory neck propagation. A small fluctuation (oscillation) first appears in the stable neck propagation and then grows into the large oscillation

0032-3861/93/112306-09

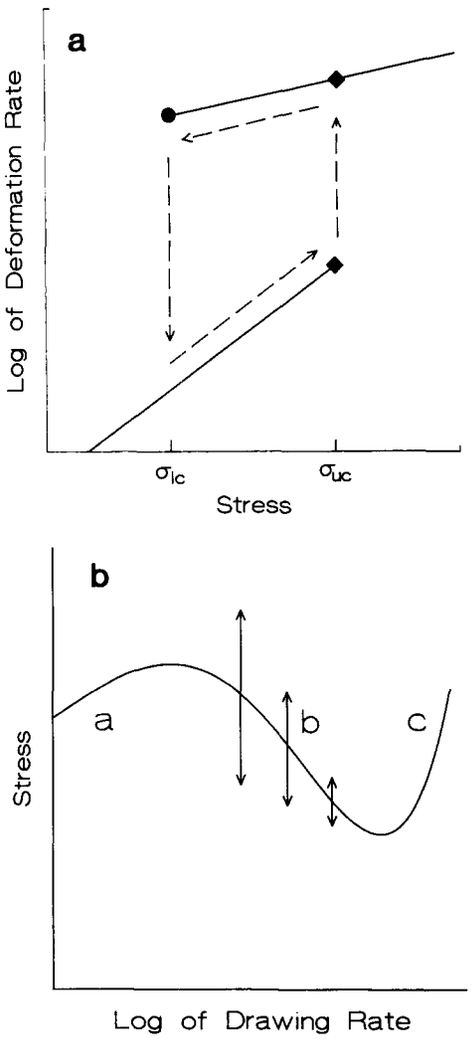

Figure 2 Schematic plot of deformation rate *versus* stress for drawing at constand load (a) and at constant speed (b). ◆, Transition found by Pakula and Fischer[3]; ●, recently Yamane *et al.*[4] found that the region of higher drawing velocity extended to lower stress. In (a), the broken arrows show a route of stress oscillation suggested in ref. 4. In (b), the double arrows represent the experimental magnitude of stress oscillation

of $d\sigma/dV<0$ disappear when the sample is immersed in water making heat dissipation easy[1]. This suggests that the process should be considered as non-isothermal.

For the first model, on the other hand, the last fact mentioned above is the premise. Further, for drawing at constant speed in the region of $d\sigma/dV<0$ ('b' in *Figure 2b*), as we shall see below, an analysis based on the model predicts stable neck propagation in the early stage and stress oscillation in the later stage. For drawing at constant load, the analysis suggests unstable neck propagation in the region of $dV/d\sigma<0$ from the initial stage of drawing, as we shall see. The instability of neck propagation in the region of $dV/d\sigma<0$ explains why the observed V–σ plot in *Figure 2a* lacks the region 'b' in *Figure 3* corresponding to 'b' in *Figure 2b*.

In this way, we can understand the behaviour of cold drawing at constant speed and at constant load, on the basis of the unified picture presented by the first model. In the following, we first discuss experiments to examine unstable neck propagation in region 'b' in *Figure 3*. Then we briefly review the first model of Barenblatt. Finally, we discuss the stability of neck propagation in the regions of $d\sigma/dV>0$ and <0 and examine oscillating solutions derived from differential equations based on Barenblatt's model. The limits of the model are also discussed.

EXPERIMENTAL

The samples used were amorphous PET films made by Toray Film and Film Products Research Laboratories; the films were 120, 300, 800 and 1000 μm thick. Rectangular strips of various sizes were cut from the films, 2–5 mm in width and 50–150 mm in length. For all the experiments described below, samples were prepared by drawing at a low rate ($\sim 40\,mm\,min^{-1}$) so as to form a neck.

For the conventional experiments of drawing at constant speed, the samples were examined with a Shimazu Auto Graph S-100 testing machine: the extension rate ranged from 7 to $600\,mm\,min^{-1}$ and could be changed continuously. Drawing at constant load was examined by measuring the extension with the eye. In order to re-examine the effect of heat dissipation, the samples were wrapped with a tissue soaked in water or silicone oil or with aluminium foil.

To confirm the instability in the region of $dV/d\sigma<0$, the equipment shown schematically in *Figure 4* was attached to the testing machine. The sample was initially drawn at constant speed by the testing machine, with velocity in the range of $d\sigma/dV<0$ ('b' in *Figures 2b* and *3*). The attached equipment allowed the neck propagation rate to become faster under the constraint of constant load adjusted by the weight. Hence, if neck propagation at the initial velocity was unstable and other stable stationary states existed for drawing at constant load, the propagation velocity could be transformed into the stable and faster velocity with the equipment under the condition of constant load. This experiment enabled the unstable neck propagation in region 'b' of *Figure 3* to be studied. The drawing velocity after the transformation was monitored by the change in voltage between the points on a Nichrome coil to which constant voltage was applied; one point was fixed and the other was in contact with a copper bar which was fastened to the moving lower clamp and glided along the Nichrome coil.

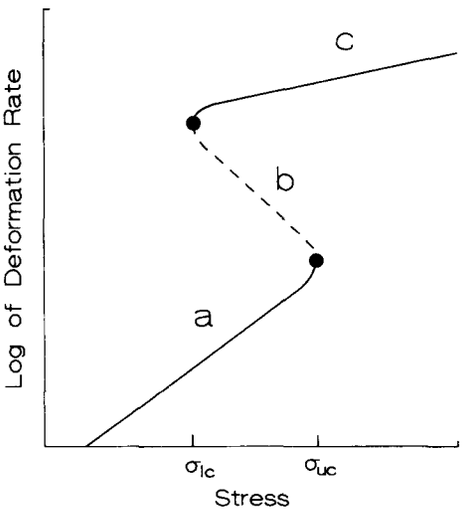

Figure 3 Hypothetical plot of deformation rate *versus* stress for drawing at constant load. A hidden unstable mode of neck propagation is expected, as indicated by the broken line

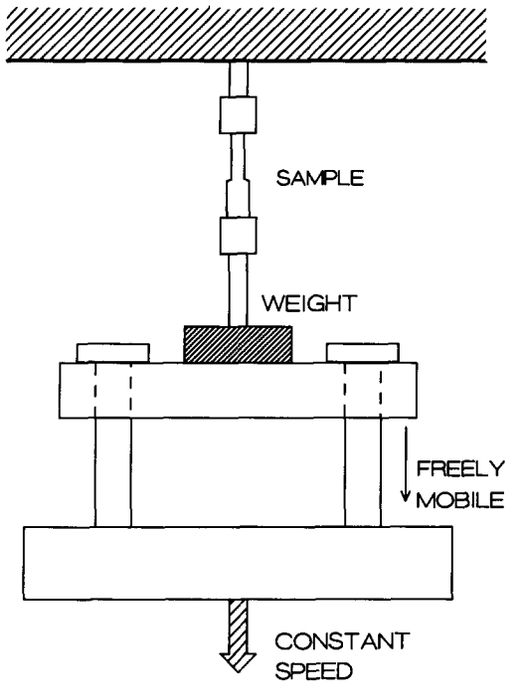

Figure 4 Schematic diagram of equipment attached to testing machine and used for examining the stability of neck propagation

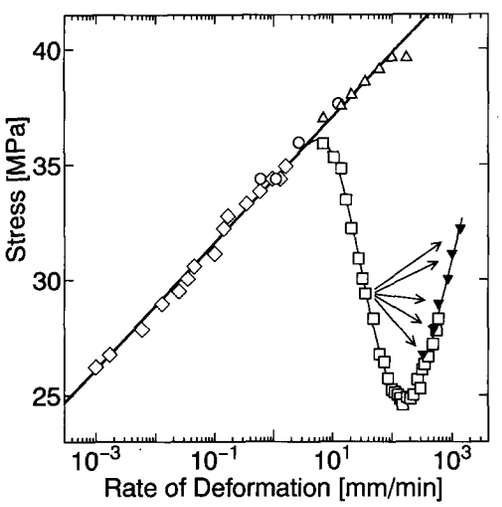

Figure 5 Plots of stress against deformation rate, obtained in the present experiments. The samples are 300 μm thick and 3 mm wide. Drawing conditions: ◇, constant load in air; ○, constant load in water; △, constant speed in water; □, constant speed in air; ▼, transformed by constant load in air as indicated by the arrows

DISCUSSION

Experimental results

The results of the experiments are shown in *Figures 5* and *6*. In *Figure 5*, the results for drawing at both constant speed and constant load are plotted on the same figure.

Conventional drawing experiments, the results of which are shown in *Figure 5*, indicate that the data lie on a single straight line except for drawing at constant speed in air, while oscillatory neck propagation occurred only in this mode. The linear plot indicates that $v \propto \exp(\text{const.}\,\sigma)$, a relation well known as the activated rate process of Eyring[5].

Water had some additional effects on the texture; in water and under strain, crazes were easily formed. But we can state that it is not the cause of the rise in stress, for the following reasons. First, the crazing must have the effect of decreasing the stress, the opposite effect to that observed in the experiment. Second, with silicone oil and even when the sample was wrapped in aluminium foil, the rise in stress was observed without being accompanied by crazing, although the rise in stress was not as great as that which occurred in water. Third, the stress returned to the original value (i.e. without water; △→□ in *Figure 5*) when the tissue soaked in water was removed from the sample; crazes had only a small effect, causing a very small fluctuation in the stress around the mean value. Hence, it is clear that the sample had not suffered any significant change due to the water. These results indicate that water, silicone oil and aluminium foil facilitate heat dissipation, and water conducted the heat most efficiently; probably, water can wet the sample well and sink into it by forming crazes.

The experiment with the attached equipment clearly demonstrated that the neck propagation in the region of $dV/d\sigma < 0$ ('b' in *Figure 3*) is unstable for drawing at constant load. In the experiment, it was observed that the velocity of neck propagation suddenly increased for the samples that were initially drawn at a rate in the region of $dV/d\sigma < 0$. The transformed rates are plotted in *Figure 5* (▼, the transformations are indicated by arrows). These data are on the extrapolated curve of the rates for drawing at constant speed (□) and hence we can say that the transformed stable neck propagation was in the same state as the necking at constant speed. The result means that the neck propagation adjusted to the initial rate in $dV/d\sigma < 0$ was unstable against fluctuations and was transformed into the faster steady state which was stable under the constant load drawing. Such fluctuations in stress can also be observed in drawing at constant speed before the neck propagation changes to the oscillatory mode. For the constant speed drawing, the fluctuation ends up in self-oscillation, as shown schematically in *Figure 1*. On the other hand, under the constraint forced by the attached equipment,

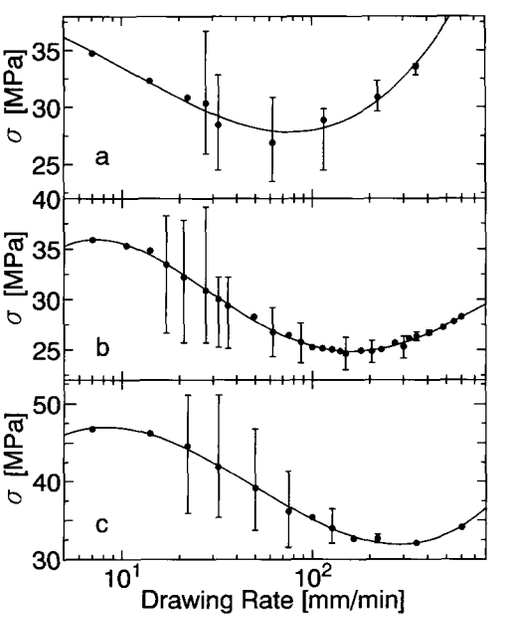

Figure 6 Plots of stress against drawing rate for samples: (a) 800 μm thick and 2 mm wide; (b) 300 μm thick and 3 mm wide; (c) 120 μm thick and 3 mm wide. The bars represent the amplitude of oscillation

the neck propagation cannot take the limit cycle and needs to be transformed to the stable state of faster necking rate; the constraint is that the stress must be larger than that decided by the weight put on the equipment.

A review of Barenblatt's model

The work of drawing converts into heat, and the heat produced will raise the temperature at the neck. For the drawing of PET films, the heat released by the work has been investigated experimentally and it was confirmed that all the work converted into heat[6]. Such an effect will have some influence on the relationship between stress and neck propagation velocity[5]. The negative $d\sigma/dV$ obtained with drawing at constant speed ('b' in *Figure 2b*) has been explained as the consequence of softening of the material due to the temperature rise expected at faster drawing rates[7].

In Barenblatt's model[2], the relationship between stress and velocity is assumed to be dependent only on the temperature and hence the physical state of neck propagation is expressed by those three parameters. This means $\sigma=\sigma(v,T)$ or $v=v(\sigma,T)$ and the physically allowed set of variables σ, v and T should be located on a surface represented by a function:

$$f(\sigma,v,T)=0 \tag{1}$$

in the three-dimensional space of (σ,v,T). It should be noted that the function, $f(\sigma,v,T)=0$, represents the σ–v relation of isothermal necking at temperature T and is therefore determined by the characteristics of neck deformation. The simplest form of this relation will be that of Eyring's rate process[5]:

$$v=v_0\exp\left(-\frac{\Delta F}{kT}\right)\left[\exp\left(\frac{\alpha\sigma}{kT}\right)-\exp\left(-\frac{\alpha\sigma}{kT}\right)\right] \tag{2}$$

where ΔF and α are the activation free energy and volume for the process and k is the Boltzmann constant; usually, a relation $\alpha\sigma/kT\gg1$ holds for the drawing of polymer materials[5].

As a measure of the neck propagation rate, Barenblatt introduced a rate, v, independent of the coordinate system;

$$v\equiv\frac{d}{dt}(l_1+l_2) \tag{3}$$

where l_1 and l_2 are the lengths of extended and unextended parts of the sample, respectively, in the unloaded state. With this rate, the rate of total deformation of the sample, V, can be expressed as:

$$v+\lambda\frac{d\sigma}{dt}=V \tag{4}$$

where λ is the elastic compliance of the whole system, which gradually becomes larger as the sample becomes elongated but, in the time interval of several periods of oscillation, can be regarded as a constant parameter because λ increases very slowly[2]. The stress σ in this equation is the apparent stress, namely $\sigma=P/S_1$ where P is the applied load and S_1 is the original cross-sectional area (*Figure 7*). Equation (4) means that the rate of the total deformation of the sample is the sum of the rates of neck propagation, v, and the elastic deformation of the sample, $\lambda(d\sigma/dt)$.

For the heat balance in the neck region, Barenblatt suggested the following equation:

$$\omega c_p\frac{dT}{dt}=Q-c_pS_2v(T-T_0)-\beta S(T-T_0) \tag{5}$$

where Q represents heat produced by the work, c_p the heat capacity of unit volume of the material, S_2 the cross-sectional area of the neck region, ω the volume of the neck region, T_0 the ambient temperature, S the lateral surface area of the neck region, and β the heat-transfer coefficient which becomes $\pi^2k/8h$ for a thin film (k is the thermal conductivity of the material and h is half the thickness of the film); the geometrical factors are shown in *Figure 7*. The first term on the right-hand side of equation (5) represents the heat produced by the work done at the neck, the second term represents the heat removed from the neck region by the propagation of the neck, and the last term represents the heat conducted from the neck region to the extended and unextended parts of the sample[2], assuming the temperature at the surface is maintained at T_0. Although Barenblatt did not give the explicit form of Q, we can derive it in a simple consideration, as follows. Since part of the total work per unit time (PV) is stored elastically in the sample [$\lambda P(dP/dt)$], the work done at the neck per unit time should be Pv and hence Q is proportional to σv.

For the convenience of the following analysis, we redefine equation (5) as follows:

$$\frac{dT}{dt}=q(\sigma,v,T) \tag{6}$$

$$q(\sigma,v,T)\equiv a\sigma v-bv(T-T_0)-c(T-T_0) \tag{7}$$

where a, b and c are positive constants. There will be an additional effect of excess heat released by, for example, crystallization, the rate of which will be a function of σ, v and T.

Equations (1), (4) and (6) form the basis of all the following analyses.

$$\frac{d\sigma}{dt}=\frac{1}{\lambda}[V-v(\sigma,T)]$$

$$\frac{dT}{dt}=q[\sigma,v(\sigma,T),T]$$

Barenblatt analysed necking at constant speed

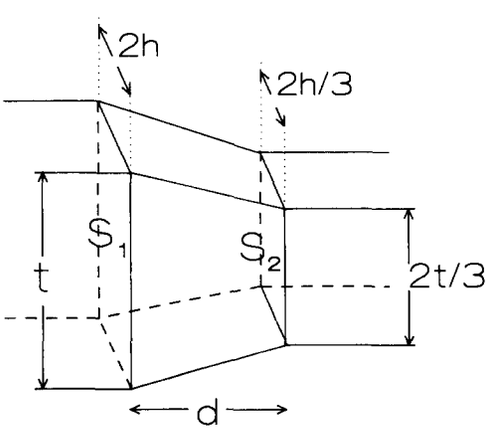

Figure 7 Schematic representation of neck region. The ratios of the width and thickness of extended part to those of unextended part are for the actual neck of PET films

(V=const.). Because of the difficulty of solving non-linear equations analytically, he analysed the stability of a stationary solution ($d\sigma/dt=0$ and $dT/dt=0$) which is represented by a point of intersection of the following surfaces in the space of σ, v and T: $f(\sigma,v,T)=0$, $v=V$ and $q(\sigma,v,T)=0$. He proved that the solution becomes unstable under a certain condition and that the unstable stationary solution changes to a limit cycle on the surface of $f(\sigma,v,T)=0$; here, $d\sigma/dt$ and dT/dt in equations (4) and (6) oscillate. He argued that the limit cycle represents the oscillatory propagation of neck.

Barenblatt has shown that the parameter determining the stability is the elastic compliance of the whole system λ. The stationary solution remains stable if $1/\lambda$ is larger than a critical value of Ω; we will have such a small λ for the early stage of drawing. The inverse of λ decreases as the sample becomes elongated and can be smaller than Ω in the late stage of drawing, when the solution becomes unstable, as observed experimentally (*Figure 1*). The critical Ω can take a positive or negative value and only when it is positive can the stationary solution be unstable:

$$\Omega \equiv (\partial_v \sigma)_*(\partial_T q)_* - (\partial_T \sigma)_*(\partial_v q)_* \tag{8}$$

where $(\partial_T\sigma)_*$ means the value of $(\partial\sigma/\partial T)_{v=\text{const.}}$ of the surface, $f(\sigma,v,T)=0$, for the stationary solution.

On the basis of the above results obtained by Barenblatt, we discuss further details of oscillatory neck propagation in the following sections.

Stability in the regions of $d\sigma/dV>0$ and <0

It can be shown that the sign of Ω is directly related to the sign of $d\sigma/dV$ and $dV/d\sigma$ in the σ–V and V–σ plots, such as those shown in *Figures 2a* and *b*:

$$\left(\frac{d\sigma}{dV}\right)_{V=\text{const.}} = \frac{\Omega}{\Psi} \tag{9}$$

$$= 1\Big/\left(\frac{dV}{d\sigma}\right)_{\sigma=\text{const.}} \tag{10}$$

$$\Psi \equiv (\partial_T q)_* + (\partial_T \sigma)_*(\partial_\sigma q)_* \tag{11}$$

where Ψ becomes negative for the form of q shown in equation (7) and for the obvious relation, $\partial_T\sigma<0$. Hence, this equation means that $d\sigma/dV$ and $dV/d\sigma$ are proportional to $-\Omega$. In the following, we discuss the stability of neck propagation in the regions of $d\sigma/dV>0$ and <0.

Drawing at constant speed. In the region of $d\sigma/dV>0$, neck propagation should always be stable because of the negative Ω. In the region of $d\sigma/dV<0$ and for the late stage of drawing ($0<1/\lambda<\Omega$), unstable neck propagation will be transformed into oscillatory propagation. These predictions satisfactorily explain the observed behaviour of oscillatory neck propagation in *Figures 1* and *2b*.

Drawing at constant load. If we neglect stability, we should have the same stationary solution for drawing both at constant speed and at constant load, and hence the V–σ and σ–V plots, as shown in *Figures 2a* and *b*, should be identical except for the stability of the solutions. Actually, *Figure 2a*, the plot of the observed steady state solutions for constant load drawing, indicates an S-shaped curve, as in the σ–V plot if *Figure 2b*, with the disappearance of the region $dV/d\sigma<0$.

For drawing at constant load, it can be shown that the sign of Ω again determines the stability of the steady state solution; here, irrespective of the value of λ, positive Ω means an unstable and negative Ω means a stable stationary solution. Therefore, the stationary solution in the region of $dV/d\sigma>0$ should be stable and the solution in the region of $dV/d\sigma<0$ must be unstable, irrespective of the value of λ. This explains why the region 'b' in *Figure 3* could not be observed before.

In the present experiment, the velocity was initially forced to the unstable value and we observed a sudden change in the velocity. As shown schematically in *Figure 3*, the hidden region of $dV/d\sigma<0$ is coexisting with the two stable regions of $dV/d\sigma>0$. Therefore, the result of the present experiment is explained as the transformation of the velocity to the faster and stable stationary state by moving along a curve of $f(\sigma_0,v,T)=0$, limited by the constant stress σ_0. Under the condition of constant load, oscillatory propagation is impossible because the locus is constrained on the one-dimensional curve $f(\sigma_0,v,T)=0$.

Oscillating solution for equations (1), (4) and (6)

In this section, we try to obtain the numerical solution for the simultaneous differential equations (1), (4) and (6). For this purpose, we need to define the surface $f(\sigma,v,T)=0$. However, at present, we have no information about the effect of crystallization which occurs in region 'c' in *Figure 2b* and during the oscillatory neck propagation[1]. In the following, we assume Eyring's rate process with single stage (equation (2)) for the relationship between σ, v and T and equation (7) for the heat balance; namely, we neglect the effect of crystallization. Then, we will see whether crystallization is crucial for oscillatory neck propagation.

The parameters in equations (2) and (7), v_0, ΔF, α, a, b and c, were determined in the following way. Firstly, the activation volume α was determined from the slope of the linear portion in *Figure 5* of the present experiment. In order to obtain v_0 and ΔF, we need to know the temperature dependence. These data were available from the experiments of Pakula and Fischer[3] (*Figure 8*). The data in *Figure 8* were for low velocity drawing (5 mm min^{-1}) so that the effect of temperature rise will be negligible. ΔF was determined from the interception with the y-axis. The value of v_0 was normalized for the present data with the determined values of α and ΔF. The values of a, b and c were estimated by using the

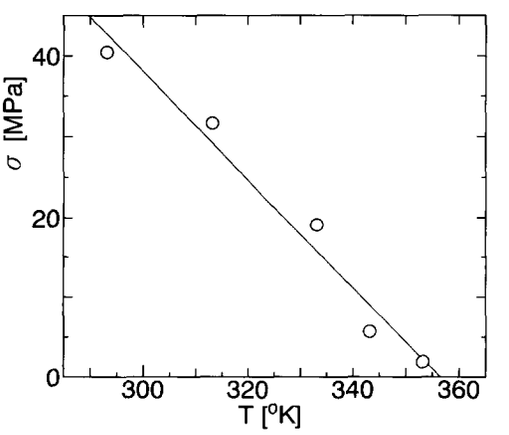

Figure 8 Plots of stress against ambient temperature. The data are from ref. 3. Cylindrical samples with diameter of 1 mm were drawn at the rate of 5 mm min^{-1}

Table 1 Constants used in the numerical calculation

v_0 (cm s^{-1})	ΔF (erg)	α (nm^3)	a (K cm s^{-1})	b (cm^{-1})	c (s^{-1})
2.25×10^{72}	8.17×10^{-12}	3.39	1.26×10^{-5}	78	13

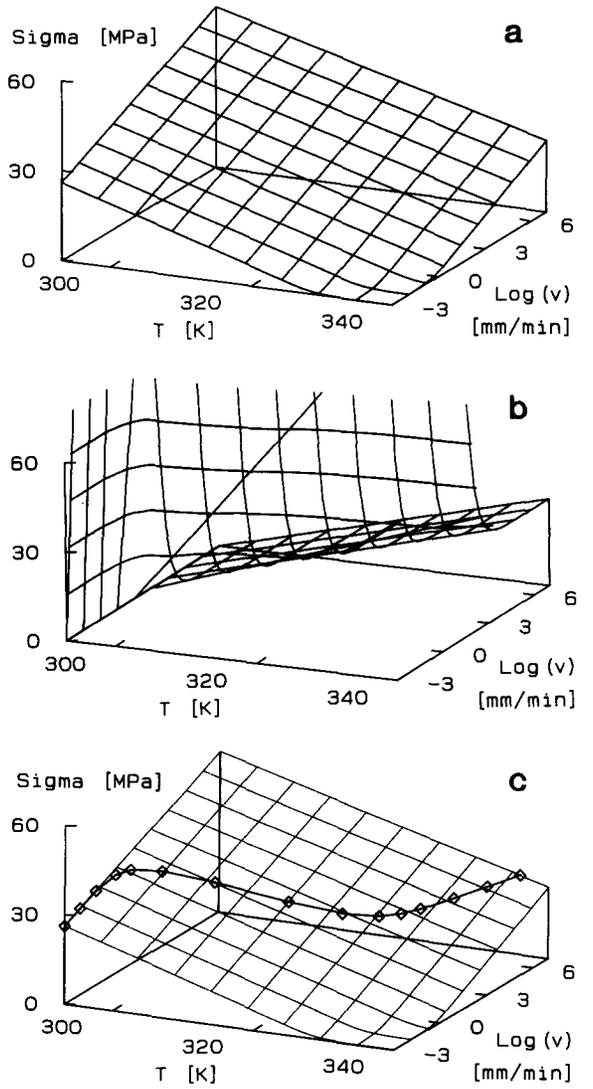

Figure 9 Three-dimensional plots of (a) equation (2); (b) $q(\sigma, v, T)=0$, (c) intersecting line of those surfaces. The intersecting line and symbols (◇) represent the steady state solution ($d\sigma/dt=0$ and $dT/dt=0$)

following values for the dimensions of the neck region (*Figure 7*) and for the physical parameters[8]: $h=150\,\mu$m, $t=3$ mm, $d=50\,\mu$m, $c_p=2.74\times10^7$ erg cm^{-3} K^{-1} and $k=1.47\times10^4$ erg s^{-1} cm^{-1} K^{-1}. These determined values are shown in *Table 1*.

First, we shall obtain the stationary solution for equations (2), (4), (6) and (7): $dT/dt=0$ and $d\sigma/dt=0$. The solutions are given by the intersecting line of the surfaces $\sigma=\sigma(V,T)$ and $q(\sigma,V,T)=0$ of *Figures 9a* and *b*, respectively, and are shown in *Figure 9c*. The σ–V plots of the solutions are shown in *Figure 10*. The plot shows an S-shaped dependence of σ on $\log(V)$. The calculated results are compared with the experimental data in *Figure 10b*, with changing the values of parameters, *a*, *b* and *c*. As seen in *Figure 10b*, the steep rise in σ with $\log(V)$ in region 'c' cannot be reproduced by the calculation. In region 'c', the extended part becomes opaque and crystallization occurs during necking. Therefore, this steep rise may be due to crystallization; although crystallization produces heat and may decrease the stress further, it will also modify the function $f(\sigma, v, T)=0$ and hence crystallization may cause hardening of the necked region and so may be able to increase the stress. Further study is required on the effect of crystallization.

Second, we shall see the time evolution of the solutions under constant speed of drawing. For this purpose, the parameter λ is kept constant. This assumption is justified because the elastic compliance of the sample increases very slowly compared to the time interval of the period of oscillation of neck propagation; we will see later, by direct numerical calculation, that the change in λ does not cause any essential difference in the results. The Runge–Kutta method with variable step size was used for the numerical calculation.

We first confirm the stable neck propagation in regions 'a' and 'c' in *Figure 10a*. The initial value of σ was set to be smaller or larger than the values for the steady states. The results shown in *Figure 11* clearly indicate stress reaching the value of the stable steady state. The stationary state was stable even with a very large value of λ ($=100$ mm MPa^{-1}).

The typical behaviour in region 'b' in *Figure 10a* ($d\sigma/dV<0, \Omega>0$) is shown in *Figure 12* for different values of λ. The critical value, $\lambda_c(=1/\Omega)$ calculated from equation (8), is 0.07 mm MPa^{-1} for the steady state. The

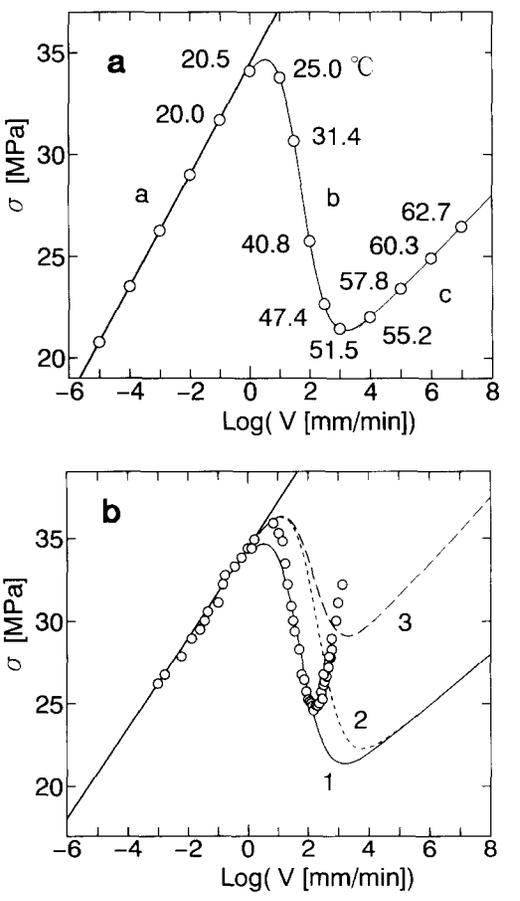

Figure 10 Plots of the stationary solutions for equations (2), (4) and (6). Temperatures at the neck are shown in (a). The curves, 1, 2 and 3 in (b) are for (*a*, *b*, *c*) shown in *Table 1*, for (*a*, *b*, 4*c*) and for (*a*, 2*b*, 4*c*), respectively. The experimental data (○) are also plotted in (b)

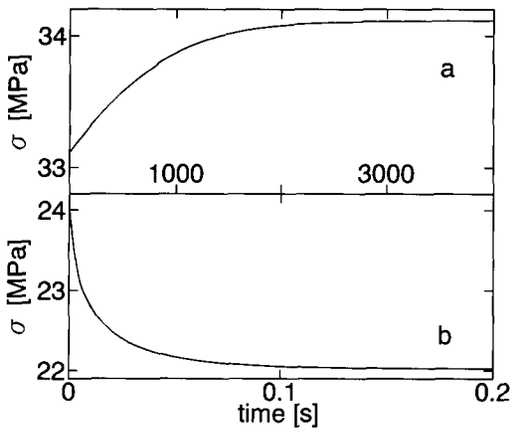

Figure 11 Plots of calculated σ as a function of time for drawing at constant speed. The drawing rates, V, are (a) 1 mm min^{-1} and (b) 10^4 mm min^{-1}. These rates are in regions 'a' and 'c' in *Figure 10a*. The values of σ are initially set to differ from the values in the steady states and the system eventually returns to the steady state

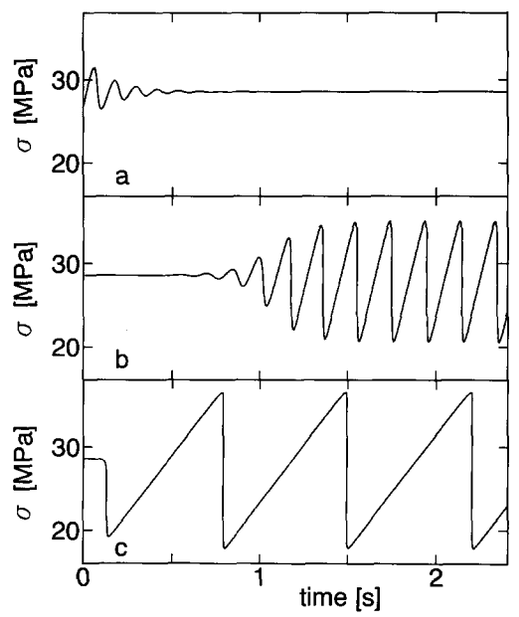

Figure 12 Plots of calculated σ as a function of time for drawing at constant speed. The rate of drawing is 50 mm min^{-1} in region 'b' in *Figure 10a*. The parameter λ takes the values of 0.065, 0.09 and 0.3 for (a), (b) and (c), respectively. The critical value of λ calculated from equation (8) is 0.07 mm MPa^{-1}. In (a), the initial σ is set to differ from the steady state σ, but in (b) and (c) the initial values of (σ, v, T) are set to be the values of the steady state

stress oscillation for $\lambda > \lambda_c$ is clearly seen in *Figures 12b* and *c*. Here, in equations (2) and (7), the effect of crystallization was neglected. We see that crystallization during necking is not the necessary condition for stress oscillation, but it will be subsidiary to quick neck propagation and its resultant temperature rise. The period of oscillation in *Figure 12* increases with λ, as was observed experimentally[1].

The changes in v and T during stress oscillation are shown in *Figure 13*. The oscillatory behaviour of σ, v and T is very similar to the experimental results of σ, v and released heat; these experimental data have been reported by Andrianova *et al.*[1,6]. The released heat is expressed as $c(T-T_0)$ in equation (7) and hence is proportional to the increase in temperature.

The limit cycle of the self-excited oscillation is plotted in *Figure 14* where a trajectory from the unstable stationary state is also shown. The cycle is clockwise and the symbols (◇) divide the limit cycle by an equal time interval; the process of increasing σ occurs very slowly compared to that of decreasing σ. As shown in *Figure 14b*, the limit cycle can be divided into four sections by the curves (1) $v=V$, and (2) $q(\sigma, v, T)=0$. The points of

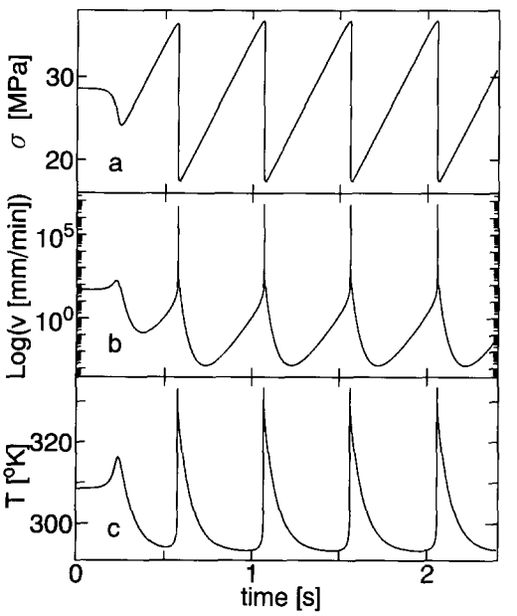

Figure 13 Plots of calculated σ, log(v) and T as a function of time. The rate of drawing is 50 mm min^{-1} in region 'b' in *Figure 10a*. The parameter λ is 0.2 and is larger than the critical value of 0.07

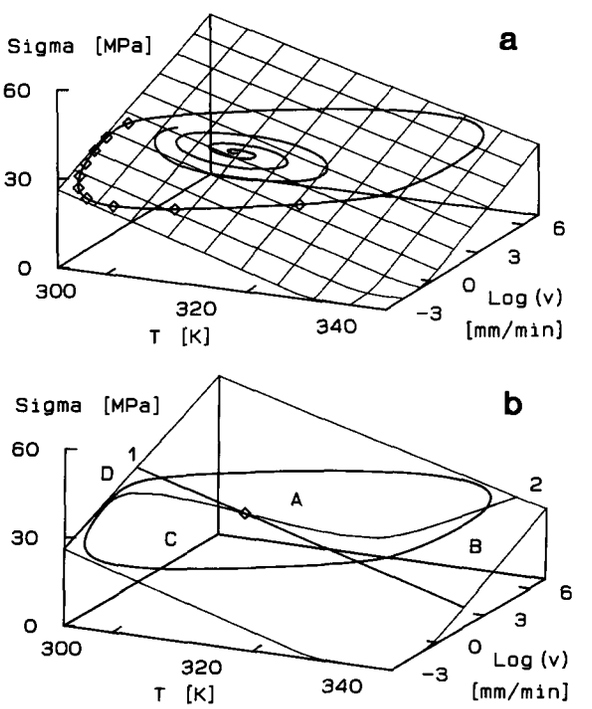

Figure 14 Three-dimensional plots of calculated σ, log(v) and T for the same drawing rate and λ as in *Figure 13*. The loop represents a limit cycle repeated in a clockwise direction. A trajectory from the unstable steady state is also shown in (a). The symbols (◇) in (a) divide the limit cycle by an equal time interval. The curves 1 and 2 in (b) represent $v=V$ ($d\sigma/dt=0$) and $q(\sigma, v, T)=0$ ($dT/dt=0$) on the surface of equation (2). In the regions A, B, C and D in (b), the signs of $(d\sigma/dt, dT/dt)$ are $(-,+)$, $(-,-)$, $(+,-)$ and $(+,+)$, respectively

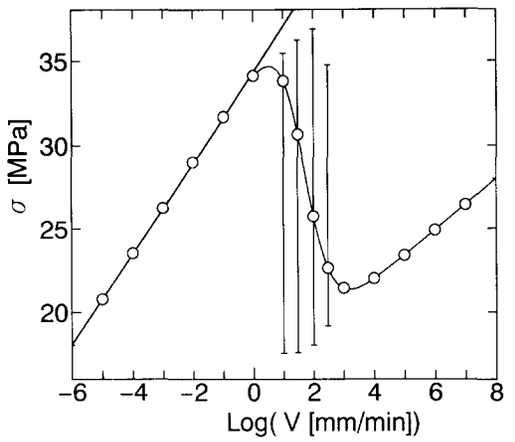

Figure 15 Plots of the amplitude of stress oscillation obtained by calculations

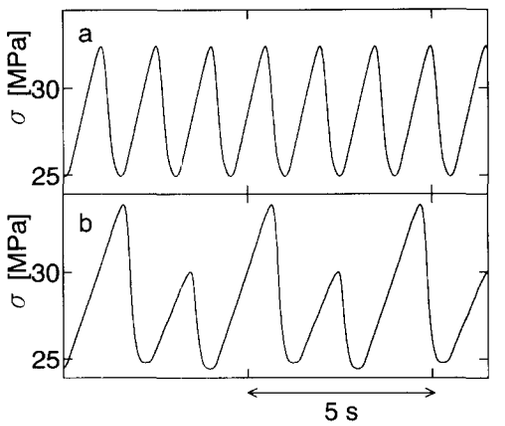

Figure 16 Typical oscillatory behaviour in stress. The sample is 1000 μm thick and 3 mm wide. The early stage of stress oscillation is shown in (a) and the later stage in (b). The change in the period and the occurrence of period doubling are clearly seen

intersection of the limit cycle with those curves represent (1) $d\sigma/dt=0$ and (2) $dT/dt=0$. The sign of $d\sigma/dt$ and dT/dt changes alternately for each section and this change maintains the limit cycle.

The amplitude of oscillation in σ is obtained for several drawing velocities and is plotted in *Figure 15*. The amplitude is almost independent of V. The change in the amplitude has been clearly observed experimentally (*Figures 2b* and *6*) but could not be reproduced by the present calculations. The change in the amplitude may be due to the effect of crystallization, which was neglected in the calculation. However, it may also be possible that Barenblatt's model itself has an essential defect for explaining the experimental result, as discussed in the following.

Limits of Barenblatt's model

1. As clearly seen in *Figure 6* especially for thicker samples, oscillatory necking is also observed for $d\sigma/dV>0$, although the present analysis based on Barenblatt's model can predict oscillation only in the region of $d\sigma/dV<0$.
2. As reported by Andrianova *et al.*[1], the period of oscillation doubles in the late stage of drawing, namely for large λ (*Figure 16*). Such period doubling can be expected for a dynamic system having more than three independent variables[9], but cannot be expected for the present model in which σ, v and T are related by the function, $f(\sigma, v, T)=0$, so that only two variables are independent. It should be noted that the system may degenerate into a chaotic mode for still larger λ by way of a successive period doubling[9].

This evidence, especially the latter, indicates the following two possibilities. First, at least one more variable may exist and at least three variables are independent. The second possibility is that the relation $f(\sigma, v, T)=0$ does not hold for the oscillatory propagation of the neck, although the relation explains the stationary neck propagation. Such mechanisms may also cause the change in the amplitude of oscillation shown in *Figures 2b* and *6*.

The parameter λ, which was kept constant in the above calculation, may be a candidate for the additional variable causing period doubling, because it gradually increases with extension of the sample. To see the effect of the increase in λ, we solve the simultaneous differential equations (2), (4), (6) and (7) with the following equation:

$$\frac{d\lambda}{dt}=\lambda_0 v \tag{12}$$

where λ_0 is a constant. The typical result is shown in *Figure 17*. We can see that the oscillation starts for λ greater than $1/\Omega\,(=0.07\,\mathrm{mm\,MPa^{-1}})$ and the period becomes longer with increasing λ. However, we could not see the period doubling or any essential differences from the results given above. We need to seek other possibilities.

Even though the above evidence is beyond the scope of Barenblatt's model, the present analysis provides a good explanation of the basic feature of the oscillatory propagation and will remain correct in a restricted sense; none of the above can be explained by the second model mentioned in the Introduction. Further investigations, both theoretical and experimental, are required along the lines of Barenblatt's model.

CONCLUSIONS

Barenblatt's model of oscillatory neck propagation has been briefly reviewed. The model comprises equations describing both the characteristics of isothermal neck propagation and heat balance in the neck region. For

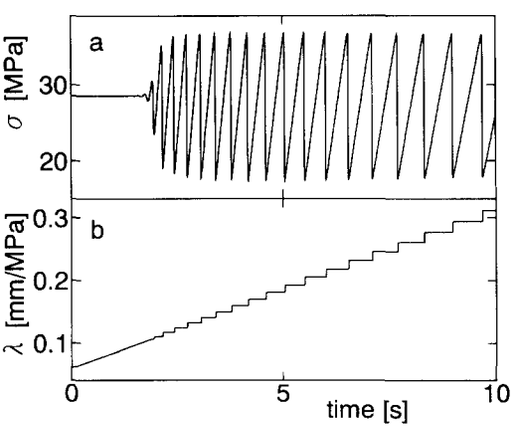

Figure 17 Plots of calculated σ as a function of time. In the calculation, the parameter λ changes according to equation (12), where the constant λ_0 is set to 5.0×10^{-5}. The drawing rate is 50 mm min^{-1} and the critical λ is 0.07

drawing at constant speed, the additional condition of maintaining constant speed is also required. Oscillatory neck propagation is described as a self-excited oscillation generated by the coupling of elastic deformation of the sample and the temperature-dependent velocity of neck propagation.

On the basis of Barenblatt's model, the stability of neck propagation has been discussed in connection with the slope of the σ–V plot. It has been shown that neck propagation becomes unstable in the region of negative slope. For drawing at constant speed, the stability is also dependent on the elastic compliance of the system and the oscillatory neck propagation starts in the later stage of necking. For drawing at constant load, neck propagation in the unstable region is unsteady from the initial stage of necking. For constant load drawing, oscillatory neck propagation is impossible because of the constraint of the constant load, and hence drawing in the unstable region is not observed by conventional experiments.

The unstable neck propagation in the region of negative slope in the V–σ plot by constant load drawing has been examined experimentally by a conventional testing machine modified to allow change in neck propagation velocity while keeping a constant load. The velocity was initially forced to be in the unstable region and the instability was clearly confirmed by observation of a sudden change in the neck propagation velocity to a faster and stable mode.

Simultaneous non-linear equations based on Barenblatt's model have been derived and solved numerically. The steady state solutions gave an S-shaped curve for the σ–V plot and, in the region of negative slope, the time development of solutions showed self-excited oscillation in stress, neck propagation velocity and temperature. These results reproduce well the experimental results reported in the literature, although the equations neglect the effect of crystallization which occurs at high drawing rates and during oscillatory necking. This means that crystallization during necking will be a subsidiary effect to temperature rise by high drawing rates.

The present analysis clarifies the basic feature of oscillatory neck propagation but cannot explain all the experimental results. First, the steady state solution could not reproduce the steep rise in stress required in the σ–V plot at high drawing rate. Second, the numerical solutions did not exhibit strong dependence of the amplitude of stress oscillation on drawing rate. Third, the well known behaviour of period doubling in stress oscillation cannot be obtained by the present system. It is probable that some of these can be explained by the effect of crystallization which was neglected in the present analysis; experimental studies with non-crystalline samples are required to investigate this issue. On the last point, however, Barenblatt's model may have an essential defect.

ACKNOWLEDGEMENTS

The author thanks Mr Deguchi of Toray Film and Film Products Laboratories for the kind supply of PET films. The author is also grateful to Drs H. Miyaji and K. Izumi for discussions. This work was partly supported by a Grant-in-Aid for Scientific Research from the Ministry of Education, Science and Culture of Japan.

REFERENCES

1 Andrianova, G. P., Kechekyan, A. S. and Kargin, V. A. *J. Polym. Sci., A-2* 1971, **9**, 1919
2 Barenblatt, G. I. *Mech. Solids* 1970, **5**, 110
3 Pakula, T. and Fischer, E. W. *J. Polym. Sci., Polym. Phys. Edn.* 1981, **19**, 1705
4 Yamane, T., Umemoto, S., Okui, N. and Sakai, T. *Polym. Prep. Japan.* 1991, **40**, 1284
5 Ward, I. M. 'Mechanical Properties of Solid Polymers', Wiley, New York, 1971, Ch. 11
6 Andrianova, G. P., Arutyunov, B. A. and Popov, Yu. V. *J. Polym. Sci., Polym. Phys. Edn* 1978, **16**, 1139
7 Allison, S. W. and Ward, I. M. *Br. J. Appl. Phys.* 1967, **18**, 1151
8 Lawton, E. L. and Ringwald, E. L. 'Polymer Handbook' (Eds J. Brandrup and E. H. Immergut), Wiley, New York, 1989, p. V-101
9 Haken, H. 'Advanced Synergetics', Springer-Verlag, Berlin, 1983, Ch. 1